POLITECNICO DI TORINO
Repository ISTITUZIONALE

Greener RAN operation through machine learning

Original
Greener RAN operation through machine learning / Vallero, G., Renga, D., Meo, M., Marsan, M.A.. - In: IEEE TRANSACTIONS ON NETWORK AND SERVICE MANAGEMENT. - ISSN 1932-4537. - (2019). [10.1109/TNSM.2019.2923881]

Availability:
This version is available at: 11583/2750034 since: 2019-10-17T12:27:01Z

Publisher:
Institute of Electrical and Electronics Engineers Inc.

Published
DOI:10.1109/TNSM.2019.2923881

Terms of use:

This article is made available under terms and conditions as specified in the corresponding bibliographic description in the repository

Publisher copyright

(Article begins on next page)

07 October 2026

Greener RAN operation through machine learning

Greta Vallero, Daniela Renga, Michela Meo, Marco Ajmone Marsan
Department of Electronics and Telecommunications, Politecnico di Torino, Italy

***Abstract*—The use of base station (BS) sleep modes is one of the most studied approaches for the reduction of the energy consumption of radio access networks (RANs). Many papers have shown that the potential energy saving of sleep modes is huge, provided the future behavior of the RAN traffic load is known. This paper investigates the effectiveness of sleep modes combined with machine learning (ML) approaches for traffic forecast. A portion of a RAN is considered, comprising one macro BS and a few small cell BSs. Each BS is powered by a photovoltaic (PV) panel, equipped with energy storage units, and a connection to the power grid. The PV panel and battery provide green energy, while the power grid provides brown energy. Our study examines the impacts of different prediction models on the consumed energy mix and on QoS. Numerical results show that the considered ML algorithms succeed in achieving effective trade-offs between energy consumption and QoS. Results also show that energy savings strongly depend on traffic patterns that are typical of the considered area. This implies that a widespread implementation of these energy saving strategies without the support of ML would require a careful tuning that cannot be performed autonomously and that needs continuous updates to follow traffic pattern variations. On the contrary, ML approaches provide a versatile framework for the implementation of the desired trade-off that naturally adapts the network operation to the traffic characteristics typical of each area and to its evolution.**

***Index Terms*—Radio access network, traffic prediction, machine learning, energy efficiency, power consumption, renewable energy, energy storage.**

I. Introduction

THE attention of the networking research community to the amount of energy necessary to run the Internet was raised by the seminal paper by Gupta and Sing, published 15 years ago [1]. This trailblazing research work spurred a very popular research line, with the involvement of many research groups around the world.

We can classify the results that have come out of these numerous research efforts in two domains. The first refers to network-level resource management algorithms, that exploit temporal and spatial variations of traffic loads to achieve energy efficiency through the use of sleep (or Low Power Idle) modes [2]. Sleep modes reduce the amount of active networking equipment to the minimum necessary to provide the desired capacity to serve the instantaneous traffic demand while keeping the desired QoS level. The second domain refers to improvements of the energy characteristics of the telecommunication equipment themselves [3], aiming to reduce power consumption through the use of low-power components, the adoption of more efficient power amplifiers, the increase of the thermal operation range to reduce the need for cooling, etc.

The results in the latter domain have been largely adopted by Mobile Network Operators (MNOs), and are contributing to the better energy efficiency of new generations of networks. For example, BSs of 3G systems had a typical peak power consumption of about 3.5 kW, while newer 4G BSs can consume less than 1 kW.

On the contrary, one of the main MNO's concerns for the adoption of dynamic resource management algorithms based on sleep modes is the fear that an excessive number of on/off transients can increase the number of faults in the network, and that unexpected QoS degradation can occur if network traffic is not correctly predicted.

As a result, the energy consumption of telecommunication networks keeps increasing at a remarkable speed, around 12% a year [4]. This is not surprising, considering that the number of mobile devices and the capacity required by applications running on them have grown extremely fast during the last years and will increase even further, as reported in [5], that forecasts that mobile data traffic will grow at a compound annual rate of 47% until 2021.

Energy saving approaches are thus more necessary than ever, and while equipment manufacturers keep improving the efficiency of their machines, it is necessary to devise viable approaches to resource management algorithms based on sleep modes.

If the reduction of the absolute value of energy consumption of telecommunication networks seems unrealistic, it is surely possible to aim at a reduction of the amount of energy necessary to transfer a unit of data (or to cover a given area, or to reduce latency to the desired level), and to the differentiation of the type of energy that is consumed. Indeed, a recent trend in networking is to consider the availability of energy produced by Renewable Energy Sources (RES), and to optimize the use of this "green" energy with respect to the energy taken from the power grid, which can be considered "brown", since it is largely produced by burning fossil fuels.

In this paper we focus on the energy consumption of a portion of a RAN comprising one macro cell and a few small cells, equipped with a small renewable energy (RE) generator to power the BSs, and an energy storage unit to cope with the intermittent nature of RE production.

While RES can reduce operational costs by reducing the amount of energy that has to be purchased from the power grid, they typically are not sufficient to make the RAN portion self-sufficient due to the limitations in the size of photovoltaic (PV) panels or wind wheels imposed by the environment in which BSs are installed (often in urban or suburban areas). Therefore, RES generation has to be combined with resource management strategies that exploit the fact that the traffic demand in a RAN portion varies over time, presenting peaks for relatively short periods, and long periods of resource under-utilization that can translate into waste of energy. Resources on Demand

(RoD) strategies are hence needed to dynamically adapt the available resources to the current traffic demand. While during traffic peaks all the available resources must be activated, when the traffic demand is low, unnecessary BSs are switched in sleep mode. As an alternative, we can base adaptation on the availability of green energy, with an approach that is called RoPE (Resources on Produced Energy).

The combination of RE generation and RoD/RoPE strategies was already proved very effective in optimizing radio resource usage and in minimizing operational costs [6], [7], [8]. However, these works make the optimistic and unrealistic assumption that both the future traffic demand and the future RES production are exactly known.

In this paper, we overcome this unrealistic assumption and consider a scenario in which network operation is decided based on traffic and energy generation predictions that are derived from ML algorithms trained with past traffic and energy production patterns. The estimation of traffic demand is clearly extremely critical: if traffic is underestimated, BSs deactivation may lead to QoS deterioration; conversely, if traffic is overestimated, lower energy saving than possible is achieved. In our approach, starting from real data, the future traffic load and RES production are forecast. Strategies which aim at reducing the network power consumption are then applied according to the forecasts.

Our key contribution is to provide a clear understanding of the effects on network operation of the introduction of ML algorithms for the forecast of future traffic and RES production. The general conclusions that come out of our investigation are that a large error in the traffic forecast does not always imply an increase in the power consumption of the network or a deterioration of QoS. Moreover, many of the considered ML algorithms succeed in achieving a very good trade-off between energy consumption and QoS. The limited differences among ML algorithms suggest that simpler ones should be preferred, so as to reduce computational cost and simplify the collection of training data.

The paper is organized as follows. In Section II, some related work is reviewed. The scenario and the methodology of our study are discussed in Section III. Results and comparisons among ML algorithms are discussed in Section IV. Conclusions are drawn in Section V.

II. Related Work

Many works consider RE power supply for the BSs of wireless access networks. Indeed, RE sources are widely adopted in real implementations to make communication networks more energy efficient and to reduce the electricity bill [9], [10], [11]. Various papers address the critical issue of properly dimensioning RE generation systems to power mobile networks [12], [13], [14]. The sizing process entails trading off self-sustainability, cost and feasibility constraints due to the installation of a RE generation system. In [12], the problem of a proper dimensioning of the PV panels is investigated via simulation, whereas authors in [13] and [14] deploy models to derive the optimal RE system dimensioning for powering a BS. In [13] the predefined constraint on the worst month outage probability is considered, whereas in [14] costs are minimized taking into account the limit on the maximum allowed battery depletion probability. The application of RoD strategies may help to make the mobile network consumption more load proportional, thus allowing to reduce the capacity of the required RE generators and to increase the feasibility of the RE powering system. For an overview of the RoD strategies to dynamically adapt the available radio resources to the current traffic demand see [2], [15], [16]. Various studies are currently available related to the application of RoD strategies based on BS sleep modes to renewable powered mobile networks. Depending on the objectives, various sleep mode based algorithms can be applied for managing the radio resources [6], [8], [17], [18], [19], [20], [21], [22]. In [6], RoD strategies are exploited to adapt the energy consumption to the actual traffic load, in order to reduce the grid energy demand and to limit the operational cost. In [17] an ON/OFF switching algorithm, based on reinforcement learning, is deployed to optimize the self-sustainability of RE powered small cells in mobile networks. Authors of [18] propose a framework to efficiently allocate spectrum resources to users and, at the same time, switch off unneeded BSs, in order to minimize power consumption. Authors of [19] propose a time-varied probabilistic ON/OFF switching algorithm to be applied in cellular networks. In [20], [21], RoD strategies are applied in a green mobile access network to improve the interaction with the smart grid in a demand response framework, with the purpose of reducing the electricity bill and to provide ancillary services. Closely related to this paper are our previous works in [7], [8], [22], [23]. In [7], Deruyck et al. propose a capacity-based deployment tool for the design of energy-efficient wireless access networks. This tool is used in [8] to investigate a wireless access network powered by a PV panel system, where capacity responds to the instantaneous traffic demand. Moreover, it introduces additional sleep mode periods for the BSs, in case of renewable energy shortage. In [22], the effectiveness of various energy-aware RoD strategies, based on BS sleep modes, is compared, trading off the reduction of the on-grid energy demand and the provided network capacity. Furthermore, analytical models are deployed to predict the green network performance as a function of PV panel size and storage capacity. In [23], the micro BSs enter sleep mode according to energy price: when the energy is expensive, the micro BSs are deactivated. Therefore, the network energy consumption decreases, as well as the cost needed to buy from the grid the amount of energy that is needed for the RAN supply.

In the literature, a lot of effort has been put in time series forecasting. An ARIMA and a Seasonal ARIMA (SA) models are used in [24] and [25], respectively, for the prediction of mobile data traffic. These works demonstrate the high accuracy of these two methods, but also their need of slow training and forecasting that makes them impractical for on-line forecasting. To provide faster forecasting and better prediction accuracy, Artificial Neural Networks (ANN) are widely exploited. In [26], an ANN is applied to the short-term load forecasting of hourly electric loads, which present similar characteristic of the traffic demand. Indeed, they vary

during the day, according to human activities: they assume low values during the night but high values during the day. For this reason, they present daily and weekly periodicity. The paper distinguishes two distinct patterns (week-day and week-end patterns), which are trained separately, using historical data. In [25] and [27], Cortez et al. find out that the ANN provides promising results in the forecast of the hourly amount of traffic in TCP/IP networks. In [28], the authors introduce an hybrid scheme, structured in an ANN and a Recurrent Neural Network (RNN). The network forecasts the solar energy for the home energy management system. A RNN is also used in [29], [30], [31]. In [29], it is used for the prediction of the hourly down-link average throughput. In [30], very good performance is reached in the forecast of the mobile traffic of an LTE BS, using 1 ms resolution data. In [31], high accuracy is achieved with a RNN, to predict the traffic. Forecast samples are employed for the optimization of the resources allocation in an optical network. Least Squares Support Vector Machine (LS-SVM) are used in [32], for the traffic demand prediction. With the same aim, in [33], the authors propose a Block Linear Regression (BLR) model, which exploits the periodicity, the spatial similarity and the short term variability of the traffic patterns. This methodology is characterized by low complexity, since a single model, based on the linear regression is trained for all BSs. Andrade et al. in [34] propose Gradient Boosting Trees for the prediction of the renewable energy production, giving as input features extracted from a numerical weather prediction grid.

III. Methodology

In this paper we look at portions of a Long Term Evolution-Advanced (LTE-A) RAN. Each RAN portion offers services over a specific service area, and consists of one cluster comprising one macro BS that defines a cell over the whole service area, and a few micro BSs that define small cells providing additional capacity in hot spots within the service area during peak traffic demand. Thus, the small cells area coverage overlaps with the coverage of the macro cell.

The cluster operates by using power provided by a RES, typically a PV panel, and an energy storage (one or more batteries); this is the green energy component of the cluster. The BSs use green power generated by the PV panel; if extra energy is produced, it is stored in the battery, while if additional energy is needed to power the BSs, it is drained from the battery. Additionally, a connection to the power grid is available, to survive periods of insufficient or no RES production and empty battery; this is the brown energy component of the cluster. Hence, brown energy is used if the energy generated by the PV panel and the one stored in the battery are not enough to power the BSs. The cluster is schematically represented in Fig. 1.

In order to reduce the brown energy consumption, so as to obtain both a reduction in energy cost, and a more energy parsimonious network operation, the centralized Network Management System (NMS) predicts the future traffic demand in the cluster as well as the future RES production. Based on these predictions, the NMS applies some resource management strategy.

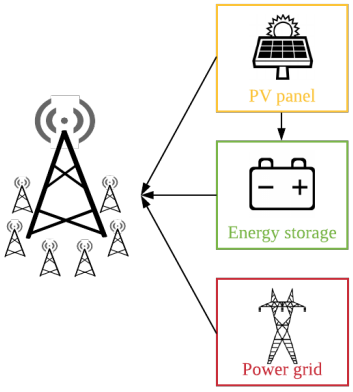

Fig. 1. A cluster composed by one macro BS and a few micro BSs is powered by the PV panel, the battery and the power grid.

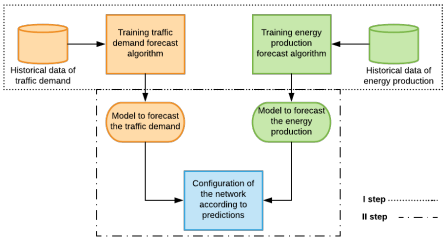

Fig. 2. Flowchart of the two-step network operation.

As shown in Fig. 2, the NMS operation consists of 2 steps:

1) **Training phase**. The algorithms used to predict the RE production (green shapes in Fig. 2) and the traffic demand (orange shapes in the figure) are trained using historical data.
2) **Run-time phase**. At the beginning of each time slot (that we assume to last 1h), the RE production and the traffic demand are forecast. Given the two predictions, the network is operated according to the implemented power saving strategy (blue shape in Fig. 2).

We consider two strategies for power saving. The **Resource on Demand (RoD)** strategy proposed in [6] aims at minimizing the network energy consumption by adapting the network capacity to the traffic demand: when traffic is low, one or more micro cell BSs are put to sleep mode and their corresponding traffic is carried by the macro cell. In practice, at the beginning of each time slot, the micro cell BSs which verify both the following conditions, are put in sleep mode:

- The forecast traffic load of the considered micro cell BS is lower than the threshold ρ_{min}. The threshold ρ_{min} is such that, when traffic is above ρ_{min}, moving traffic from the micro cell to the macro cell is not convenient in terms of power consumption. The threshold is set according to the value suggested in [6] (ρ_{min} = 0.37).
- The capacity of the macro cell BS is enough to carry the traffic of the considered micro cells.

The second strategy, **Resource on Produced Energy (RoPE)**, is implemented by adapting the procedure used in [8].

The micro cell BSs are switched off if the local available green energy is not enough to power the BSs of the cluster and the macro cell can carry the traffic of the micro cells. In particular, when the amount of available green energy (produced and stored) is lower than the energy necessary to operate the cluster in the next time slot, the micro cell BSs are switched off gradually, provided their traffic can be managed by the macro cell, until the available green energy becomes sufficient to operate the cluster in the next time slot.

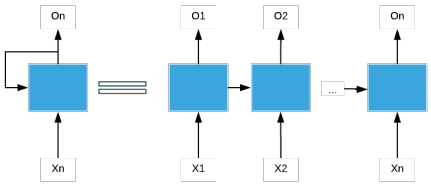

Fig. 3. Scheme of the Long Short Term Memory Cell (LSTMC).

A. Traffic prediction

For the prediction of the traffic load of each BS we consider and compare a number of machine learning techniques.

1) Block Linear Regression: BLR is proposed in [33] to forecast the traffic demand in wireless communication networks. This predictor reflects the daily and weekly periodicity of mobile traffic, and is formulated using linear regression. A single model is constructed to forecast the traffic of all the considered BSs, starting from the past traffic data of all BSs.

2) Artificial neural network: The Artificial Neural network (ANN) model proposed in [26] is used, considering separate ANNs for each BS. Each ANN is composed of 4 layers: the input layer which has 5 nodes, 2 hidden layers with 4 nodes each, and the output layer with one node. The traffic prediction is obtained by feeding 5 past traffic samples as input. As in [26], the input features are chosen according to the daily periodicity of the traffic and to the high correlation between consecutive samples. In more detail, to predict the traffic demand of BS *b* at hour *t* of day *d*, the following values are given as input to the network:

- $T_{b,d,t-1}$: traffic on BS *b* at hour *t-1* of day *d*;
- $T_{b,d-1,t}$: traffic on BS *b* at hour *t* of day *d-1*;
- $T_{b,d-1,t-1}$: traffic on BS *b* at hour *t-1* of day *d-1*;
- $T_{b,d-2,t}$: traffic on BS *b* at hour *t* of day *d-2*;
- $T_{b,d-2,t-1}$: traffic on BS *b* at hour *t-1* of day *d-2*.

Four different prediction methods are considered; for each BS:

- 1 ANN is used, without distinction between week-day and week-end traffic patterns;
- 24 ANNs are separately trained, one per each hour of the day;
- 2 ANNs are separately trained, one for the week-day traffic pattern and the other for the week-end pattern;
- 48 ANNs are separately trained, 1 for each of the 24 hours of the week-day traffic pattern and the remaining 24 for each of the 24 hours of the week-end pattern.

When the distinction between week-day and week-end patterns is considered, the inputs of the ANN, which belong to past days, are taken from the corresponding pattern. Therefore, the samples of past days of a week-end day (or a week-day) are taken in the previous week-end days (or a week-day).

3) Long Short Term Memory Cell (LSTMC): In this case, a RNN is trained for each BS. This kind of neural network is called recurrent since the output of the hidden layers is fed back into the network itself, as shown in Fig. 3, in which on the right part we show the unrolled version of what the left part shows [29].

As in [29], the RNN is obtained with a single LSTMC layer. An LSTMC has an internal memory state which is added to the processed input. Therefore, the cell is responsible for remembering and computing the value of the state.

4) Baseline: In order to assess the effectiveness of the prediction approaches presented above, we need to compare their performance against some simple baseline cases. The simplest baseline estimation consists in computing for each BS the average traffic demand for each hour, and in using such average as the predictor. In particular, for BS *b*, an hourly predictor for week-days and an hourly predictor for week-ends are computed with the traffic samples belonging to the training dataset:

$$\overline{T}_{b,t} = \frac{1}{D}\sum_{d=0}^{D} T_{b,d,t}, \qquad t = 0, 1, ..., 23 \tag{1}$$

where $T_{b,d,t}$ is the traffic demand at the BS *b* at time interval *t* of day *d* and D is the number of days available for the training phase, in the pattern considered (week-day or week-end). The traffic demand on BS *b* at hour *t* of day *d* is forecast using the t^{th} sample of the baseline of *b*:

$$\hat{T}_{b,d,t} = \overline{T}_{b,t} + D_{b,d,t} \tag{2}$$

where $D_{b,d,t}$ is the difference between the baseline and the actual traffic demand of base station *b* at time *t* of day *d*. The estimation of $D_{b,d,t}$ is given by:

$$D_{b,d,t} = K \cdot std_{b,t} \tag{3}$$

where K is a scalar parameter set to achieve always at least 90% of carried user data in a slot, and $std_{b,t}$ is the standard deviation at time *t* on BS *b*.

5) Baseline with ANN: This prediction algorithm is similar to the previous one, but differs in the way in which the estimation of $D_{b,d,t}$ is computed. In this case, $D_{b,d,t}$ is forecast using an ANN. To forecast the traffic demand of BS b at hour t of day d, the ANN inputs are the following:

- $\overline{T}_{b,t} - T_{b,d,t}$: difference on BS *b* between the baseline and the actual traffic demand at hour *t-1* of day *d*;
- $\overline{T}_{b,t} - T_{b,d-1,t}$: difference on BS *b* between the baseline and the actual traffic demand at hour *t* of day *d-1*;
- $\overline{T}_{b,t} - T_{b,d-1,t-1}$: difference on BS *b* between the baseline and the actual traffic demand at hour *t-1* of day *d-1*;
- $\overline{T}_{b,t} - T_{b,d-2,t}$: difference on BS *b* between the baseline and the actual traffic demand at hour *t* of day *d-2*;
- $\overline{T}_{b,t} - T_{b,d-2,t-1}$: difference on BS *b* between the baseline and the actual traffic demand at hour *t-1* of day *d-2*.

B. Forecast of the energy produced by the PV panels

The amount of the energy produced at time *t* is predicted using linear regression, giving as input the following features:

- month, day, current hour,
- average of the beam irradiance at time *t-1* (W/m^2),
- average of the diffuse irradiance at time *t-1* (W/m^2),
- average of the ambient temperature at time *t-1* (°C),
- average of the wind speed at time *t-1* (m/s) ,
- average of the plane of array irradiance at time *t-1* (W/m^2),
- average of the PV cell temperature at time *t-1* (°C)

C. Performance indicators

The effectiveness of the prediction algorithms is evaluated in terms of the following Key Performance Indicators (KPIs):

- **AMARE (Average Mean Absolute Relative Error),** which measures the average ratio between the real and predicted traffic patterns. It is computed as:

$$AMARE = \frac{1}{B}\sum_{b=1}^{B} MARE_b \tag{4}$$

where B is the number of the considered BSs and $MARE_b$ is the MARE (Mean Absolute Relative Error) on BS b, derived by:

$$MARE_b = \frac{1}{D \cdot H}\sum_{d=1}^{D}\sum_{t=1}^{H}\frac{|T_{b,d,t} - \hat{T}_{b,d,t}|}{T_{b,d,t}} \tag{5}$$

where $T_{b,d,t}$ is the real traffic demand at time *t* of day *d* on BS *b*, $\hat{T}_{b,d,t}$ is the forecast traffic demand at time *t* of day *d* on BS b, D is the number of days (and of the testing phase) and H is 24. When AMARE refers to the difference between the real and predicted energy generation by RES, it is computed as:

$$AMARE = \frac{1}{D \cdot H}\sum_{d=1}^{D}\sum_{t=1}^{H}\frac{|E_{d,t} - \hat{E}_{d,t}|}{E_{d,t}} \tag{6}$$

where $E_{d,t}$ is the real renewable energy production at time *t* of day *d*, $\hat{E}_{d,t}$ is the forecast renewable energy production at time *t* of day *d*, D is the number of days (and of the testing phase) and H is 24;

- **AME (Average Mean Error) is an error metric defined as:**

$$AME = \frac{1}{B}\sum_{b=1}^{B} ME_b \tag{7}$$

where B is the number of the considered BSs and ME_b (Mean Error) on BS b is derived as:

$$ME_b = \frac{1}{D \cdot H}\sum_{d=1}^{D}\sum_{t=1}^{H}(T_{b,d,t} - \hat{T}_{b,d,t}) \tag{8}$$

where $T_{b,d,t}$ is the real traffic demand at time *t* of day *d* on BS *b*, $\hat{T}_{b,d,t}$ is the forecast traffic demand at time *t* of day *d* on BS b, D is the number of days of the testing phase, and H is 24. In the AME, negative and positive values are possible; indeed, AME indicates whether the considered algorithm systematically overestimates or underestimates the traffic: When the AME is positive, the algorithm tends to underestimate the traffic demand, while in case of negative values of the AME, the traffic is usually overestimated. AME is complementary to AMARE which is a measure of the prediction error in absolute terms. The AME indicator can be derived for the difference between the real and predicted energy generation by RES:

$$AME = \frac{1}{D \cdot H}\sum_{d=1}^{D}\sum_{t=1}^{H}(E_{d,t} - \hat{E}_{d,t}) \tag{9}$$

where $E_{d,t}$ is the real renewable energy production at time *t* of day *d*, $\hat{E}_{d,t}$ is the forecast renewable energy production at time *t* of day *d*, D is the number of days (and of the testing phase) and H is 24;

- **Overall energy consumption** of the BS cluster, considering that in each time slot some BSs are active and consume energy, while some others are in sleep mode and consume no energy;
- **Average capacity** of the BS cluster, again considering that in each time slot some BSs are active and provide capacity, while some others are sleeping and do not provide capacity;
- **Percentage of lost traffic**, i.e., the percentage of traffic demand that cannot be carried by the network, again accounting that in each time slot some BSs are active and manage the traffic demand, while some others are sleeping and do not provide any service. This metric is used as measure of the QoS in the considered RAN.

The performance indicators obtained using the traffic and energy predictions provided by the proposed algorithms are compared to each other. In addition, they are compared with the performance of the *Reference Scenario* that consists of an always ON approach in which all the BSs are always active regardless the amount of traffic demand and produced energy. Moreover, the achieved results are compared with the *Ideal Case* in which the energy saving strategy (RoD or RoPE) is applied, according to the perfect knowledge of the future traffic demand and the future energy production.

D. Input Data

In our study we use traffic data provided by a large Italian MNO. They report the hourly traffic volume at 1420 BSs, in the city of Milan and in a wide area around it, for a duration of two months in 2015. As shown in Fig. 4, we start by considering eight portions of the city. These areas were selected for being quite different in terms of their typical activities and, hence, traffic patterns. All together, the selected areas are quite representative of the various zones that coexist in a urban environment. The Duomo di Milano area (orange square in Fig. 4) is a turistic area, with high activity levels during several hours of the day. A part of a business neighborhood (dark green) and some residential streets (yellow) are considered: the traffic in these areas follows the typical behavior of people in their daily life. In the business area traffic peaks are observed during the central hours of the day, whereas in the residential area a traffic rise is observed in the evening. The train station

TABLE I
VALUES OF THE PARAMETERS OF THE CONSUMPTION MODEL FOR MACRO AND MICRO BSS.

BS type	N_{trx}	P_{max} (W)	P_0 (W)	Δ_p
Macro	6	20	84	2.8
Micro	2	6.3	56	2.6

area (purple) is instead characterized by intense activity levels, especially at the beginning and at the end of the working hours. The San Siro neighborhood includes the soccer stadium (grey), and the activity here is quite bursty and variable depending on the possibility that events are held or not. The Politecnico di Milano area (light green) hosts a large campus with several students. The industrial zone (magenta) is a particular case of a business area, and, finally, the Rho Fiere district (brown in the figure) is an area that hosts big events, fairs and exhibitions, that might last for a few days. In each of these portions of the RAN we assume that one macro BS and 6 micro BSs are present, so that the service area is covered by one macro cell that overlaps with 6 small cells. After having investigated the performance of the considered ML approaches in support of network management decisions for these eight areas, we will look also into other areas, to make our conclusions more robust.

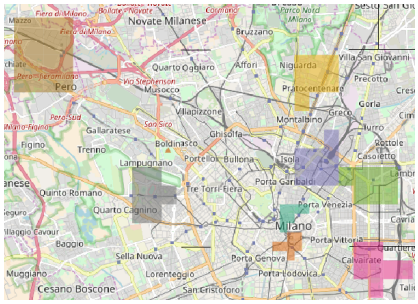

Fig. 4. Considered traffic areas: the Duomo di Milano (orange), a business (dark green), a residential (yellow), the train station (purple), the San Siro (grey), the Politecnico di Milano (light green), an industrial (magenta) and the Rho Fiere (brown) areas.

The input power required for the operation of a BS, denoted as P_{in}, is derived according to the linear model proposed in [35]:

$$P_{in} = N_{trx} \cdot (P_0 + \Delta_p P_{max} \rho), \qquad 0 \leq \rho \leq 1 \qquad (10)$$

where N_{trx} is the number of transceiver, P_0 represents the power consumption when the radio frequency output power is null, Δ_p is the slope of the load dependent power consumption, ρ is the traffic load and P_{max} is the maximum radio frequency output power at maximum load. Table I summarizes the value of the parameters for macro and micro BSs [35]. The consumption of the BS in sleep mode is considered negligible.

The energy generated by the PV panel is used to power the BSs and, in case of extra production, is fed into the batteries. When no green energy is available, the BSs use the brown energy provided by the traditional power grid (see Fig. 1). Data about RE production in Milan are estimated using the PVWATT tool [36]. The PVWATT data are derived based on realistic solar irradiation patterns, corresponding to the typical meteorological year in the considered area, with a granularity of one hour. The main typical losses occurring in a real PV system during the process of solar radiation conversion are taken into account. In our work, the PV panel system has capacity of 10 kWp. Lead-acid batteries are considered for energy storage. Each element has capacity 200 Ah and voltage 12 V. The storage capacity, defined as the number of battery units, is equal to 5. A maximum Depth of Discharge (DOD) of 70% is considered in this study. This DOD value allows the battery to operate for more than 500-600 cycles before being replaced [37], [38]. Losses of 25% in energy efficiency due to the charging and discharging processes are considered [39].

IV. RESULTS

In this section, we compare the accuracy of the traffic prediction algorithms and we investigate their effectiveness when introduced in the resource management strategies of the considered RAN portions. The data of 47 days (out of the 61 for which we have data) are used for the training phase, while the remaining 14 days are used for the run-time phase.

A. Comparison among ML algorithms

Fig. 5 reports the results of the application of the RoD strategy coupled with the various traffic forecast algorithms, in each one of the 8 considered RAN portions. The plot of Fig. 5a shows the energy consumption values, distinguishing the green (lighter) and the brown energy used. The radar plot of Fig. 5b reports the corresponding energy consumption reduction, computed with respect to the reference scenario, in which no action is taken to reduce energy consumption. Fig. 5c shows the percentage of lost traffic.

The figure indicates that, in all the considered areas, the benefit of the proposed approach is significant, with energy saving up to 40% and never below 10%. Most of the energy is produced locally by PV panels, and only a small amount, between 8% and 23%, is purchased from the power grid, typically during night, when energy is cheaper. Comparing the effectiveness of the different algorithms, results indicate that, with all the considered traffic forecast algorithms, except for the Baseline with and without ANN, energy consumption is very close to the ideal case (where we assume perfect knowledge of future traffic demand). The Baseline with and without ANN show the highest and the lowest energy consumption drops, respectively. From Fig. 5c we see, however, that energy reduction is achieved at the cost of QoS deterioration. With the exception of the Baseline with ANN, the other ML algorithms have equivalent performance within each zone, with QoS deterioration that depends on the area but is usually below 5%. When BLR, LSTMC and one or more ANNs are used, differences among the network performance indicators are limited, so that these approaches can be considered equivalent. Even if one of them may provide a more energy consuming configuration during some hours, it will provide a less energy consuming one during others.

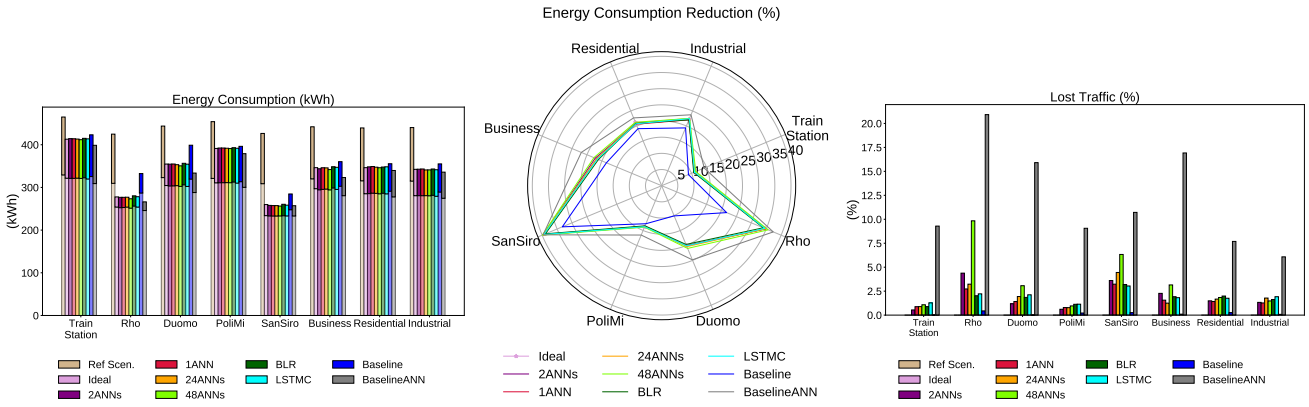

(a) (b) (c)

Fig. 5. Comparison of the effectiveness of prediction techniques under RoD: (a) Energy consumption, (b) Energy consumption reduction, (c) Percentage of lost traffic.

Observe now in Fig. 6 the AMARE (i.e., the error of the ML algorithms in predicting the traffic). AMARE is, in general, quite small. Interestingly, the Baseline, despite showing good QoS (low lost traffic), reaches 3.17 in AMARE, that is the largest error among the considered prediction techniques. This happens because for our combined energy saving and QoS goals, the correct estimation of traffic is important only around the values that are taken as thresholds for the decision to switch on or off some small cell BSs. Large errors in traffic estimations in periods of low or high traffic are irrelevant, since no network operation action is taken. This is revealed also in Fig. 7, where the hourly lost traffic and the hourly AMARE, for the Industrial zone, obtained with Baseline and 1 ANN are plotted. The figure highlights that peaks in the AMARE do not correspond to peaks of lost traffic. Indeed, at 2 a.m., the Baseline presents the maximum AMARE. Nevertheless, no traffic is lost. Moreover, even if the Baseline usually presents higher AMARE than 1 ANN, it does not provide larger lost traffic. For example, at 10 p.m., even though 1 ANN has lower AMARE than the Baseline, it causes larger lost traffic. Therefore, a larger error could not imply the deterioration of the quality of service.

Now, we analyze the pros and cons of each ML algorithm. They are reported in Table II. The table contains the number of trained models. As mentioned in Section III, a single model is trained when BLR is used. When LSTMC or the Baseline are used, a model is employed for each BS. The number of models with ANN varies: 1, 2, 24, or 48 models are needed, when 1ANN, 2ANNs, 24ANNs, or 48ANNs are used, respectively. In case of Baseline with ANN, 2 models are trained for each BS. Increasing the number of trained models, the computational power and time increase. Moreover, the table includes the adaptability to variation of each traffic pattern. It means that when a traffic pattern modifies for example its mean value, the ML algorithm is able to detect this variation. In Fig. 8a, a traffic trace which changes its mean value in time is plotted, as well as the predicted samples obtained with each considered forecast algorithm. The figure shows that the Baseline and the Baseline with ANN are not able to follow the actual trace. This is because the Baseline does not use recent samples for the forecast of the current one. The table also indicates if hyperparameters are needed for the considered algorithm. When ANNs or the LSTMC are used, the number of hidden layers, as well as the number of neurons for each layer should be decided. If the Baseline and the BLR are chosen, no hyperparameters are needed. Therefore in these two cases, the design of the model is easier.

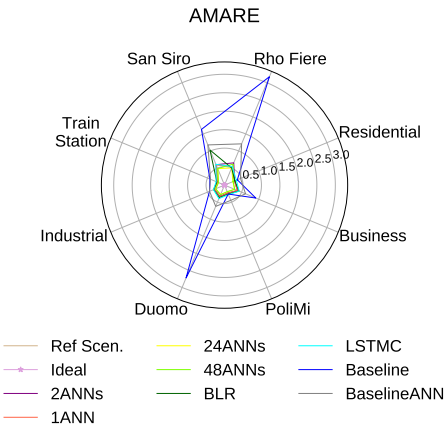

Fig. 6. AMARE of the traffic forecast algorithms.

TABLE II
PROS AND CONS OF EACH ML ALGORITHM.

ML algorithm	Number trained models	Adaptability to variation	Hyper parameters
1 ANN	1 for each BS	Yes	Yes
2 ANNs	2 for each BS	Yes	Yes
24 ANNs	24 for each BS	Yes	Yes
48 ANNs	48 for each BS	Yes	Yes
BLR	1	No	No
LSTMC	1 for each BS	Yes	Yes
Baseline	1 for each BS	No	No
Baseline with ANN	2 for each BS	No	Yes

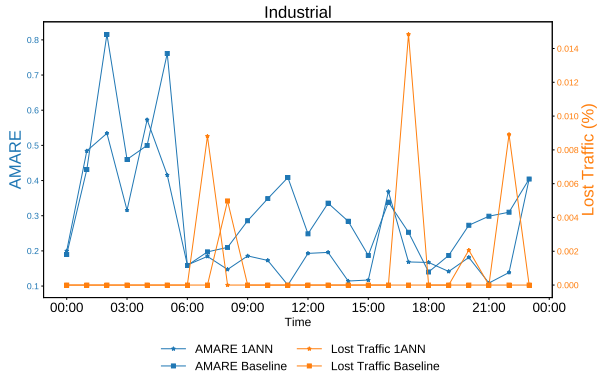

Fig. 7. Hourly AMARE and hourly lost traffic in the Industrial zone

B. Impact of traffic patterns

We now investigate the impact of traffic patterns. As already visible in the previous figures, there is quite some difference among the performance indicators in the various geographical areas. To better catch this, Fig. 9 combines energy consumption and lost traffic by representing each prediction algorithm in each area with a marker positioned so that the x-axis value corresponds to the energy consumption and the y-axis value corresponds to the percentage of lost traffic. We clearly see that results are clustered according to the geographical area. The area-dependent behavior derives from the traffic patterns that characterize the areas. The Train Station and PoliMi areas have a typical traffic demand which is larger than the threshold for many hours (around 40% of the test phase). Because of this, the energy consumption can not be reduced significantly (Fig. 5b), since each BS is needed to carry the traffic and cannot enter sleep mode. In the Business, Duomo, Residential and Industrial zones the traffic pattern is larger than the threshold for shorter periods than in the previous case. For this reason, the RoD strategy results more effective in terms of energy consumption reduction, as can be seen in Fig. 5b. The average (among all ML algorithms) AMARE in the Industrial area increases by 23% with respect to the one given by the Train Station area (Fig. 6). Nevertheless, Fig. 5c reveals that the lost traffic is almost the same: around 1.9%, on average. This results from different average distances from the threshold. Indeed, in the Train Station area the average distance of the hourly amount of traffic is approximately $7.8 \cdot 10^{10}$ bit, while in the Industrial zone it is larger than $10 \cdot 10^{10}$ bit. Thus, even presenting larger AMARE, an incorrect deactivation is less frequent thanks to the large distance from the threshold, preventing the deterioration of the QoS. Finally, the RAN portions that we called San Siro and Rho Fiere exhibit the most favorable patterns, with long periods of low traffic demand. This leads to the largest reductions of energy consumption (see Fig. 5b). Thus, in these areas, during the day, the traffic demand is usually lower than the threshold. Nevertheless, these areas present sometimes unpredictable and random very high peaks which result in the largest AMARE and the worst QoS (Fig. 5b, 6). Because of the shortness of the duration of the data trace, the prediction models can not learn these peculiar and irregular behaviours.

We now consider two quite different areas: Rho Fiere and Duomo. Figs. 10a and 10b highlight the inter-relations among the different performance indicators obtained with RoD, using different traffic demand forecast algorithms in each area. As expected, the performance in the two areas is significantly different for all indicators. This means that a widespread implementation of energy efficient strategies without the support of ML algorithms would require a complex tuning of the network management algorithms. In addition, since traffic patterns change with time, a careful adaptation to these variations would also be necessary. An automatic learning process of the traffic patterns, and a consequent automatic tuning of the energy efficiency strategies, are clearly necessary.

We can again observe that higher values of AMARE do not always imply higher energy consumption or worse QoS. Indeed, energy consumption and amount of lost traffic depend on the configuration of the network, which can be correct (i.e., the same as in the ideal case), even with a large error in the traffic forecast.

The average capacity of the considered RAN portion, which depends on the average number of active BSs, and the AME, which depends on the prediction trend, provide information about the behavior of the traffic forecast algorithms. Large average capacity means that the conditions to put in sleep mode the micro BSs are verified infrequently. The same happens when negative AME is achieved. In such a case, the forecast traffic may be overestimated. On the contrary, low average capacity and positive AME indicate traffic underestimation. These trends affect QoS and energy consumption. A detailed comparison of the traffic forecasts for the areas Rho Fiere and Duomo is shown in Figs. 8a and 8b, respectively. When the Baseline algorithm is used, traffic is overestimated and, hence, the average capacity is always larger than in all other cases (blue curve in the figures) and the AME is always more negative than in all other cases (blue curve in Fig. 11). The energy consumption drops by 10% and 22%, respectively in the two areas, without any lost traffic. In the cases of BLR, LSTMC and one or more ANNs, the average capacity decreases, since the traffic is better estimated. In such a case, the AME (Fig. 11) is closer to zero. This means that the overestimated samples compensate the underestimated ones. The average capacity further decreases when the Baseline is combined with the ANN. The AME reaches large positive values, since this model underestimates traffic.

C. Comparison between strategies

We now compare the performance of the RoD and RoPE energy consumption reduction strategies.

Under the RoPE strategy, a micro BS is switched in sleep mode when the available energy is lower than the consumed one, provided that its traffic can be carried by the macro BS. This occurs rarely, if compared with the conditions for the micro BS deactivation in RoD. To show this, Fig. 12 reports the real and the forecast renewable energy generation (black and red dashed lines, respectively) and the real and forecast

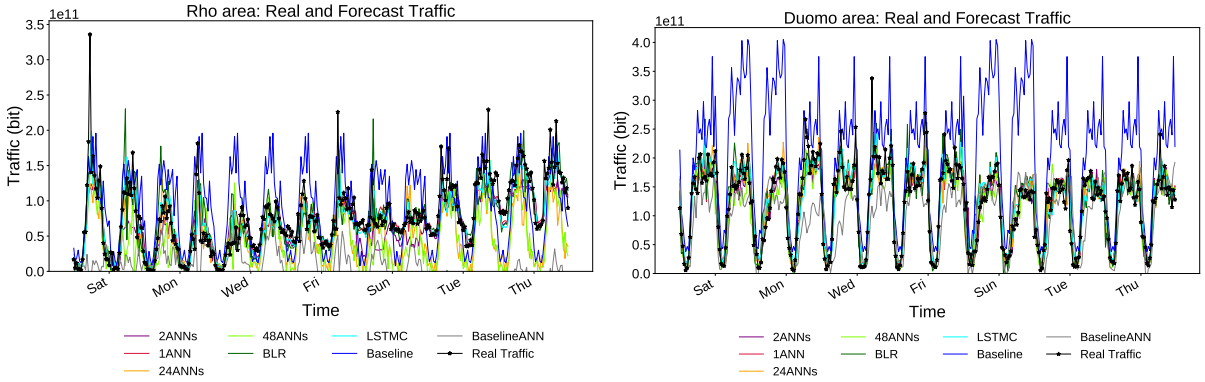

(a) (b)

Fig. 8. Forecast of the traffic demand: Rho Fiere (a) and Duomo (b)

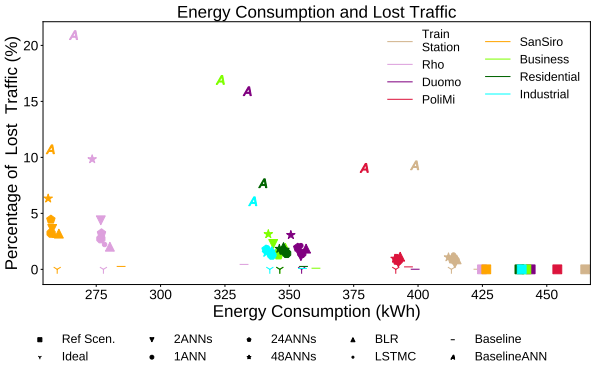

Fig. 9. Energy consumption and lost traffic, with different prediction techniques under RoD.

energy consumption in the PoliMi area, computed with the traffic predictions given by the different ML algorithms. The AMARE and the AME of the production of RES is 15 and 137 $\cdot 10^3$, respectively. Nevertheless, the estimation algorithm fails mainly in the forecast of the peaks. The predicted amount of RES production is lower than the actual value, but greater than the forecast and real power consumption. For this reason, the RAN is usually configured properly. Therefore, under the RoPE strategy, the behavior is almost the same whatever ML algorithm is used, as can be seen in Fig. 13b, which reports the number of active BSs during one day in the PoliMi area. Observe also that, under RoPE, all BSs are active for longer periods of time than under RoD (Fig. 13).

Fig. 14 reports the energy consumption, the energy consumption reduction and the QoS achieved by RoPE using the considered ML algorithms, for all areas under analysis. An interesting aspect is that the adopted prediction model has less impact on results with RoPE with respect to RoD. By comparing the performance for RoD (Fig. 13a) and RoPE (Fig. 13b) it can be seen that the network configurations obtained with RoPE are less dependent on the used traffic forecast algorithm. Even if the Baseline algorithms give the smallest energy consumption reduction, they typically differ from the others by less than 5 percentage points. This is because the amount of available renewable energy is similar in the various scenarios, even if the traffic predictions differ. Moreover, the amount of available renewable energy is often sufficient to power the cluster, keeping all the micro BSs active (Fig. 12). During these periods, the obtained network configurations are identical, even using different traffic prediction algorithms (from 8 a.m. to 10 p.m. in Fig. 13b). This does not occur between 11 p.m. and 7 a.m., when the green energy produced by the PV panels, collected and stored in the battery during the day, is not sufficient. Part of this time interval coincides with low traffic demand periods. In this case, even with different errors in the forecast, the configurations obtained with any traffic forecast model are minimal: typically, all the micro BSs are put in sleep mode. Because of this, with RoPE, QoS is less compromised than with RoD: less than 1% of traffic is lost, see Fig. 14c.

D. *Performances evaluation over many additional areas*

The last part of this work consists in the evaluation of the KPIs obtained with the proposed methodology over 8 additional areas to test the robustness of our considerations. We use 8 new portions of the RAN that are indicated in Fig. 15. As before, each area is covered by one macro cell BS which overlaps with 6 micro cell BSs. The results are presented in Fig. 16, where the power consumption and the percentage of lost traffic are plotted, using RoD or RoPE. Each area is identified by an integer. Integers from 1 to 8 corresponds to the previously considered areas numbered according to the following order: 1 - Train Station; 2 - Rho Fiere; 3 - Duomo; 4 - PoliMi; 5 - San Siro; 6 - Business; 7 - Residential; 8 - Industrial areas. Numbers from 9 to 16 are related respectively to: 9 - an area rich of touristic attractions (orange in Fig. 15); 10 - a urban zone, including a theatre (green); 11 - a portion of the Assago village, where a famous sports facility is located (red); 12 - a residential neighborhood (magenta); 13 - an area containing a section of the highway (grey); 14 - the zone of the Milano's airport (light blue); 15 - a district in Monza city (purple); 16 - a park (brown).

Results are similar to the ones presented in the previous Sections. When RoD is used, the power consumption is

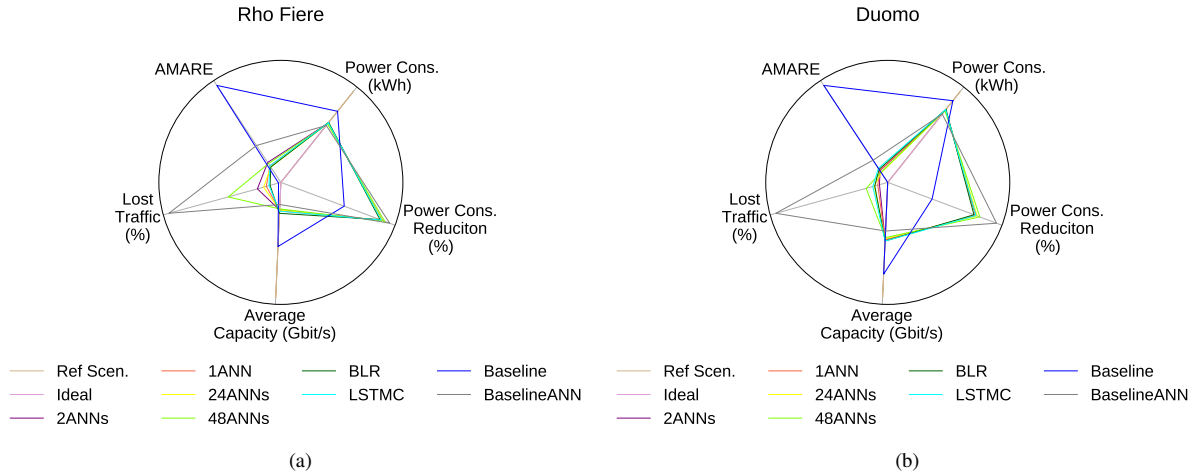

(a) (b)

Fig. 10. Comparison among performance indicators under RoD for two quite different zones: Rho Fiere (a) and Duomo (b).

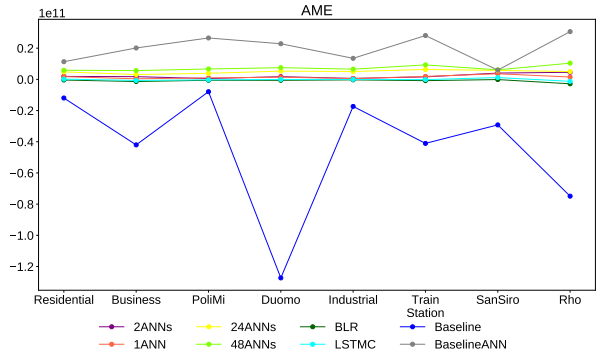

Fig. 11. AME of the traffic forecast algorithm.

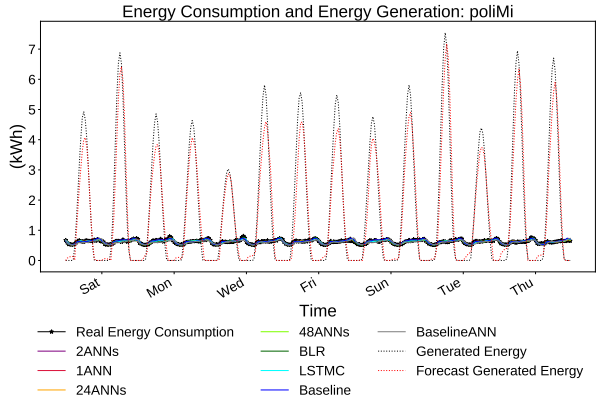

Fig. 12. Real and forecast energy generation by RES and real and forecast energy consumption.

reduced by up to 40% and never below 9% (Fig. 16a). The reduction in power consumption strictly depends on the traffic pattern. The ML algorithms do not impact power consumption, with all of them providing reductions very close to the ideal case. As shown in Fig. 16b, this reduction is achieved at the expense of a deterioration of QoS: some traffic is lost, but usually not more than 5%, except for the Baseline with ANN. As before, the Baseline combined with the ANN provides the highest power consumption reduction, but the worst QoS: up to 20% of traffic is lost (Figs. 16a, 16b).

When RoPE is chosen, the reductions in power consumption are lower, between 8% and 16% (Fig. 16c) and less dependent on traffic demand shape, for the reasons mentioned in Section IV-C. The lost traffic is usually lower than 1%, as shown in Fig. 16d.

V. Conclusion

We considered different portions of a RAN providing services in the city of Milano, each one corresponding to a cluster comprising one macro cell and 6 micro cell BSs. Each cluster is powered by a PV panel with energy storage units, which provide green energy to the BSs. The cluster is also connected to the power grid, which supplies brown energy.

We investigated the effectiveness of ML algorithms to forecast the production of green energy and the traffic demand. These forecasts drive the choice of an energy-efficient cluster configuration with either a RoD (Resources on Demand) or a RoPE (Resources on Produced Energy) approach. In particular, the energy saving approach activates the minimum number of small cell BSs necessary to satisfy the forecast traffic demand.

Our results show that large errors in the forecast do not always imply bad network performance. Indeed, the correct estimation of traffic is important only around the values that are taken as thresholds for the decision to activate or deactivate some micro cell BSs.

In addition, we observed that many of the considered ML algorithms succeed in achieving quite a good trade-off between energy consumption and QoS. Obviously, forecast algorithms that tend to overestimate traffic, yield lower energy saving without deteriorating QoS. On the contrary, forecast algorithms that tend to underestimate traffic yield losses of traffic, but higher energy saving: up to 5 percentage points more than the ideal case (which does not compromise QoS).

Our results show that when the RoPE strategy is used, the network performance does not depend much on the ML

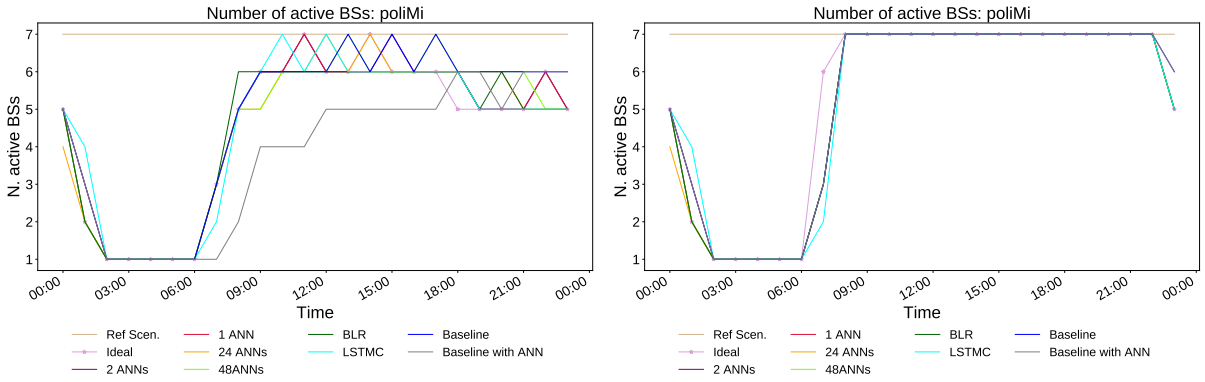

(a) (b)

Fig. 13. Number of the active BSs during a day in the train station area, using RoD (a) and RoPE (b)

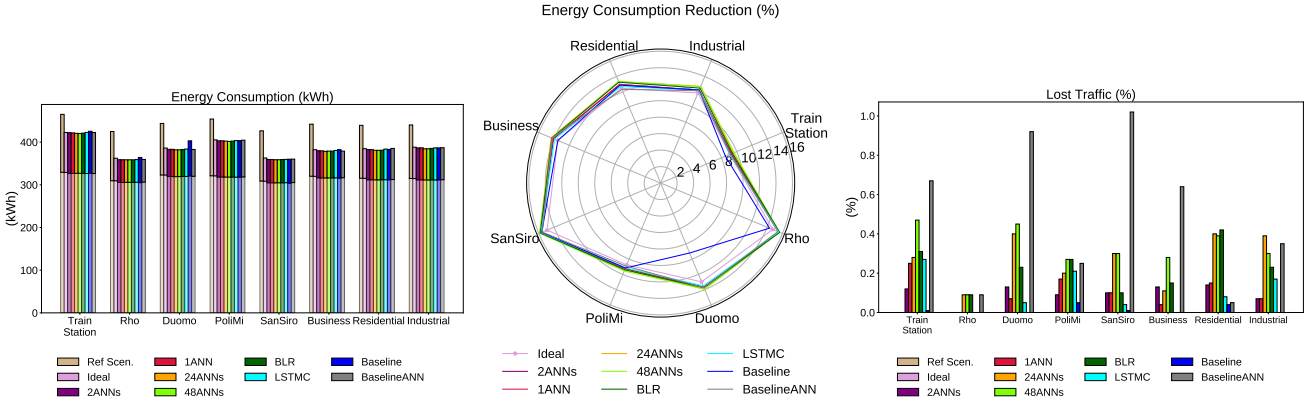

(a) (b) (c)

Fig. 14. Comparison of the effectiveness of prediction techniques under RoPE: (a) Energy consumption, (b) Energy consumption reduction, (c) Percentage of lost traffic.

algorithm used for traffic prediction. This suggests that the use of RoPE is preferable to RoD, and that a simple ML algorithm like BLR, which constructs a single model for all the BSs of all the city areas, or 1 or 2 ANNs combined with RoPE can produce a very effective and flexible approach to energy efficiency and QoS. As a future work, we plan to investigate the effect of the warm/cold season. This may provide a deeper analysis of the yearly performance of the RoPE strategy, which depends on the amount of produced renewable energy.

REFERENCES

[1] M. Gupta and S. Singh, "Greening of the internet," in *Proceedings of the 2003 Conference on Applications, Technologies, Architectures, and Protocols for Computer Communications*, ser. SIGCOMM '03. New York, NY, USA: ACM, 2003, pp. 19–26. [Online]. Available: http://doi.acm.org/10.1145/863955.863959

[2] . Budzisz, F. Ganji, G. Rizzo, M. Ajmone Marsan, M. Meo, Y. Zhang, G. Koutitas, L. Tassiulas, S. Lambert, B. Lannoo, M. Pickavet, A. Conte, I. Haratcherev, and A. Wolisz, "Dynamic resource provisioning for energy efficiency in wireless access networks: A survey and an outlook," *IEEE Communications Surveys Tutorials*, vol. 16, no. 4, pp. 2259–2285, Fourthquarter 2014.

[3] L. M. Correia, D. Zeller, O. Blume, D. Ferling, Y. Jading, I. Gdor, G. Auer, and L. V. Der Perre, "Challenges and enabling technologies for energy aware mobile radio networks," *IEEE Communications Magazine*, vol. 48, no. 11, pp. 66–72, November 2010.

[4] S. Lambert, W. V. Heddeghem, W. Vereecken, B. Lannoo, D. Colle, and M. Pickavet, "Worldwide electricity consumption of communication networks," *Opt. Express*, vol. 20, no. 26, pp. B513–B524, Dec 2012. [Online]. Available: http://www.opticsexpress.org/abstract.cfm?URI=oe-20-26-B513

[5] C. V. N. Index, "Global mobile data traffic forecast update, 2015–2020," *Cisco white paper*, 2016.

[6] M. Dalmasso, M. Meo, and D. Renga, "Radio resource management for improving energy self-sufficiency of green mobile networks," *ACM SIGMETRICS Performance Evaluation Review*, vol. 44, no. 2, pp. 82–87, 2016.

[7] M. Deruyck, W. Joseph, E. Tanghe, and L. Martens, "Reducing the power consumption in lte-advanced wireless access networks by a capacity based deployment tool," *Radio Science*, vol. 49, no. 9, pp. 777–787, 2014.

[8] M. Deruyck, D. Renga, M. Meo, L. Martens, and W. Joseph, "Reducing the impact of solar energy shortages on the wireless access network powered by a pv panel system and the power grid," in *2016 IEEE 27th Annual International Symposium on Personal, Indoor, and Mobile Radio Communications (PIMRC)*. IEEE, 2016, pp. 1–6.

[9] V. Chamola and B. Sikdar, "Solar powered cellular base stations: Current scenario, issues and proposed solutions," *IEEE Communications magazine*, vol. 54, no. 5, pp. 108–114, 2016.

[10] H. A. H. Hassan, L. Nuaymi, and A. Pelov, "Renewable energy in cellular networks: A survey," in *2013 IEEE online conference on green communications (OnlineGreenComm)*. IEEE, 2013, pp. 1–7.

[11] T. Han and N. Ansari, "Powering mobile networks with green energy," *IEEE Wireless Communications*, vol. 21, no. 1, pp. 90–96, 2014.

[12] M. Meo, Y. Zhang, R. Gerboni, and M. A. Marsan, "Dimensioning the power supply of a lte macro bs connected to a pv panel and the

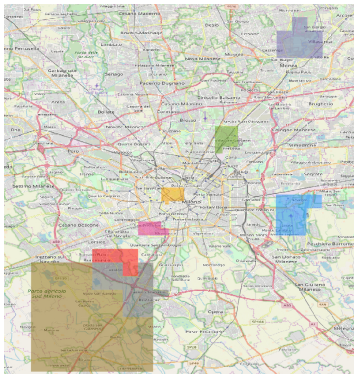

Fig. 15. Considered traffic areas: a touristic (orange), a theatre (green), a residential (magenta), a portion of Monza city (purple), the Mediolanum Forum sports facility in Assago (red), the Milano's airport (light blue), an highway (grey) and a park (brown) areas.

power grid," in *2015 IEEE International Conference on Communications (ICC)*. IEEE, 2015, pp. 178–184.

[13] V. Chamola and B. Sikdar, "Resource provisioning and dimensioning for solar powered cellular base stations," in *2014 IEEE Global Communications Conference*. IEEE, 2014, pp. 2498–2503.

[14] ——, "A multistate markov model for dimensioning solar powered cellular base stations," *IEEE Transactions on Sustainable Energy*, vol. 6, no. 4, pp. 1650–1652, 2015.

[15] T. Shankar *et al.*, "A survey on techniques related to base station sleeping in green communication and comp analysis," in *2016 IEEE International Conference on Engineering and Technology (ICETECH)*. IEEE, 2016, pp. 1059–1067.

[16] S. Buzzi, I. Chih-Lin, T. E. Klein, H. V. Poor, C. Yang, and A. Zappone, "A survey of energy-efficient techniques for 5g networks and challenges ahead," *IEEE Journal on Selected Areas in Communications*, vol. 34, no. 4, pp. 697–709, 2016.

[17] M. Miozzo, L. Giupponi, M. Rossi, and P. Dini, "Switch-on/off policies for energy harvesting small cells through distributed q-learning," in *2017 IEEE Wireless Communications and Networking Conference Workshops (WCNCW)*. IEEE, 2017, pp. 1–6.

[18] H. Ghazzai, M. J. Farooq, A. Alsharoa, E. Yaacoub, A. Kadri, and M.-S. Alouini, "Green networking in cellular hetnets: A unified radio resource management framework with base station on/off switching," *IEEE Transactions on Vehicular Technology*, vol. 66, no. 7, pp. 5879–5893, 2017.

[19] N. B. Rached, H. Ghazzai, A. Kadri, and M.-S. Alouini, "A time-varied probabilistic on/off switching algorithm for cellular networks," *IEEE Communications Letters*, vol. 22, no. 3, pp. 634–637, 2018.

[20] D. Renga, H. A. H. Hassan, M. Meo, and L. Nuaymi, "Energy management and base station on/off switching in green mobile networks for offering ancillary services," *IEEE Transactions on Green Communications and Networking*, vol. 2, no. 3, pp. 868–880, 2018.

[21] M. Ali, M. Meo, and D. Renga, "Cost saving and ancillary service provisioning in green mobile networks," in *The Internet of Things for Smart Urban Ecosystems*. Springer, 2019, pp. 201–224.

[22] M. Deruyck, D. Renga, M. Meo, L. Martens, and W. Joseph, "Accounting for the varying supply of solar energy when designing wireless access networks," *IEEE Transactions on Green Communications and Networking*, vol. 2, no. 1, pp. 275–290, 2018.

[23] G. Vallero, M. Deruyck, M. Meo, and W. Joseph, "Accounting for energy cost when designing energy-efficient wireless access networks," *Energies*, vol. 11, no. 3, 2018. [Online]. Available: http://www.mdpi.com/1996-1073/11/3/617

[24] J. Guo, Y. Peng, X. Peng, Q. Chen, J. Yu, and Y. Dai, "Traffic forecasting for mobile networks with multiplicative seasonal arima models," in *2009 9th International Conference on Electronic Measurement & Instruments*. IEEE, 2009, pp. 3–377.

[25] P. Cortez, M. Rio, M. Rocha, and P. Sousa, "Multi-scale internet traffic forecasting using neural networks and time series methods," *Expert Systems*, vol. 29, no. 2, pp. 143–155, 2012.

[26] K. Lee, Y. Cha, and J. Park, "Short-term load forecasting using an artificial neural network," *IEEE Transactions on Power Systems*, vol. 7, no. 1, pp. 124–132, 1992.

[27] P. Cortez, M. Rio, M. Rocha, and P. Sousa, "Internet traffic forecasting using neural networks," in *The 2006 IEEE International Joint Conference on Neural Network Proceedings*. IEEE, 2006, pp. 2635–2642.

[28] L. Yao and T.-S. Tsai, "Novel hybrid scheme of solar energy forecasting for home energy management system," in *2016 IEEE International Conference on Internet of Things (iThings) and IEEE Green Computing and Communications (GreenCom) and IEEE Cyber, Physical and Social Computing (CPSCom) and IEEE Smart Data (SmartData)*. IEEE, 2016, pp. 150–155.

[29] P. Torres, H. Marques, P. Marques, and J. Rodriguez, "Using deep neural networks for forecasting cell congestion on lte networks: a simple approach," in *International Conference on Cognitive Radio Oriented Wireless Networks*. Springer, 2017, pp. 276–286.

[30] H. D. Trinh, L. Giupponi, and P. Dini, "Mobile traffic prediction from raw data using lstm networks," in *2018 IEEE 29th Annual International Symposium on Personal, Indoor and Mobile Radio Communications (PIMRC)*. IEEE, 2018, pp. 1827–1832.

[31] S. Troia, R. Alvizu, Y. Zhou, G. Maier, and A. Pattavina, "Deep learning-based traffic prediction for network optimization," in *2018 20th International Conference on Transparent Optical Networks (ICTON)*. IEEE, 2018, pp. 1–4.

[32] S. Wang, J. Guo, Q. Liu, and X. Peng, "On-line traffic forecasting of mobile communication system," in *2010 First International Conference on Pervasive Computing, Signal Processing and Applications*. IEEE, 2010, pp. 97–100.

[33] H. Pan, J. Liu, S. Zhou, and Z. Niu, "A block regression model for short-term mobile traffic forecasting," in *2015 IEEE/CIC International Conference on Communications in China (ICCC)*. IEEE, 2015, pp. 1–5.

[34] J. R. Andrade and R. J. Bessa, "Improving renewable energy forecasting with a grid of numerical weather predictions," *IEEE Transactions on Sustainable Energy*, vol. 8, no. 4, pp. 1571–1580, 2017.

[35] G. Auer, O. Blume, V. Giannini, I. Godor, M. Imran, Y. Jading, E. Katranaras, M. Olsson, D. Sabella, P. Skillermark *et al.*, "D2. 3: Energy efficiency analysis of the reference systems, areas of improvements and target breakdown," *Earth*, vol. 20, no. 10, 2010.

[36] A. P. Dobos, "Pvwatts version 5 manual," National Renewable Energy Lab.(NREL), Golden, CO (United States), Tech. Rep., 2014.

[37] C. Mi and M. A. Masrur, *Hybrid electric vehicles: principles and applications with practical perspectives*. John Wiley & Sons, 2017.

[38] M. Jafari, G. Platt, Z. Malekjamshidi, and J. G. Zhu, "Technical issues of sizing lead-acid batteries for application in residential renewable energy systems," in *2015 4th International Conference on Electric Power and Energy Conversion Systems (EPECS)*. IEEE, 2015, pp. 1–6.

[39] H. Gharavi and R. Ghafurian, "Ieee recommended practice for sizing lead-acid batteries for stand-alone photovoltaic (pv) systems ieee std 1013–2007," in *Proc. IEEE*, vol. 99, no. 6, 2011, pp. 917–921.

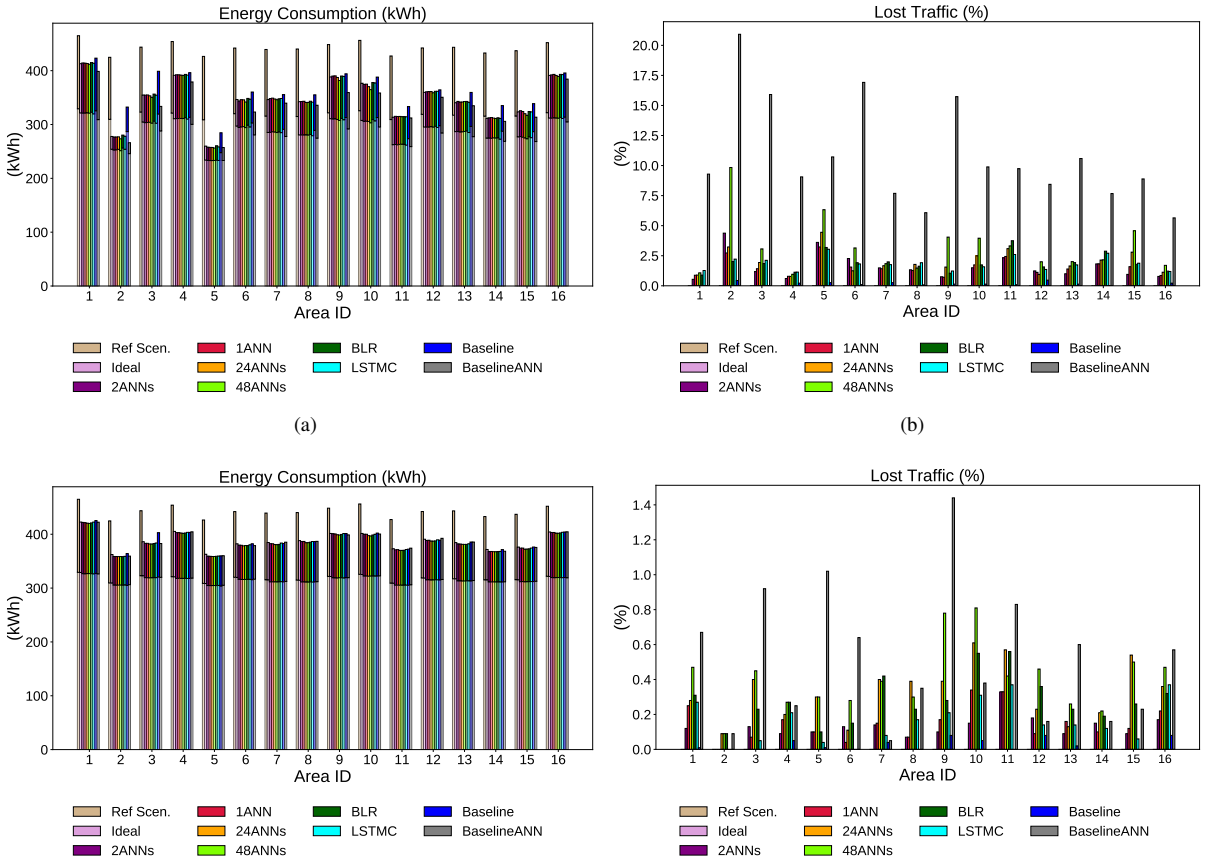

Fig. 16. Comparison of the energy consumption and the percentage of lost traffic: (a) Energy consumption with RoD, (b) Percentage of lost traffic with RoD, (c) Energy consumption with RoPE, (D) Percentage of lost traffic with RoPE.